Coalescing black hole binaries in general relativity
&
The dark matter problem in astrophysics

Alexandre Le Tiec

Gravitation et Cosmologie ($\mathcal{G}\mathbb{R}\varepsilon\mathbb{C}\mathcal{O}$)
Institut d'Astrophysique de Paris

Sous la direction de Luc Blanchet

UPMC PARIS UNIVERSITAS

IAP

École Doctorale d'Astronomie & Astrophysique d'Île-de-France

Outline

① Gravitational wave source modelling

② Post-Newtonian and self-force dynamics of black hole binaries

③ Cold dark matter and modified Newtonian dynamics

④ Dipolar dark matter and dark energy

Outline

1. Gravitational wave source modelling
2. Post-Newtonian and self-force dynamics of black hole binaries
3. Cold dark matter and modified Newtonian dynamics
4. Dipolar dark matter and dark energy

What is a gravitational wave?

A gravitational wave is a ripple in the curvature of spacetime, which propagates at the speed of light

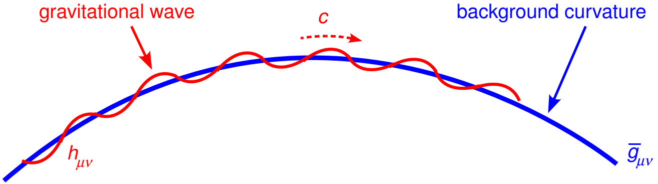

Interferometric detectors of gravitational waves (GW)

Virgo (Cascina, Italy)

High frequency band:
$10\ \mathrm{Hz} \lesssim f \lesssim 10^3\ \mathrm{Hz}$

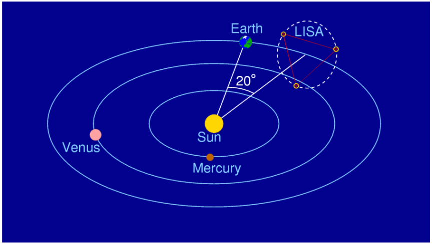

LISA (design)

Low frequency band:
$10^{-4}\ \mathrm{Hz} \lesssim f \lesssim 10^{-1}\ \mathrm{Hz}$

Main sources of GW for Virgo/LIGO and LISA

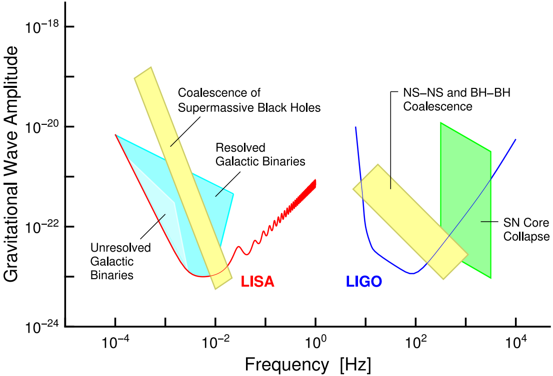

- Binary neutron stars ($M \sim 1.5 M_\odot$)
- Stellar mass black hole binaries ($M \sim 10 M_\odot$)
- Supermassive black hole binaries ($M \sim 10^6 M_\odot$)
- Extreme mass ratio inspirals (EMRIs)

Methods to compute gravitational wave templates

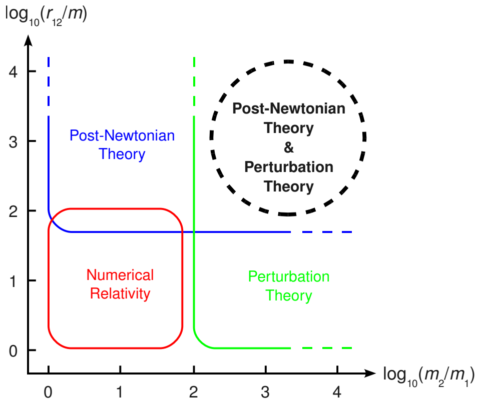

Methods to compute gravitational wave templates

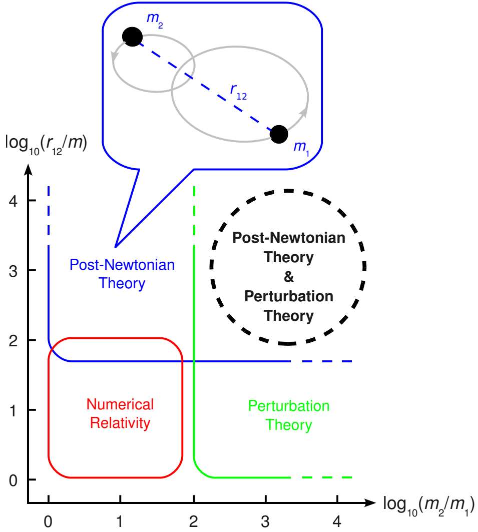

Methods to compute gravitational wave templates

The post-Newtonian (PN) formalism

Perturbation parameter

$$\varepsilon_{\mathrm{PN}} \sim \frac{{v_{12}}^2}{c^2} \sim \frac{Gm}{r_{12}c^2} \ll 1$$

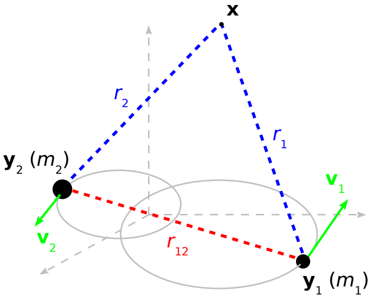

Example

$$g_{00}^{\mathrm{PN}}(\mathbf{x}) = -1 + \underbrace{\frac{2Gm_1}{r_1 c^2}}_{\text{Newtonian}} + \underbrace{\frac{4Gm_1 {v_1}^2}{r_1 c^4}}_{\text{1PN term}} + \cdots + (1 \leftrightarrow 2)$$

Methods to compute gravitational wave templates

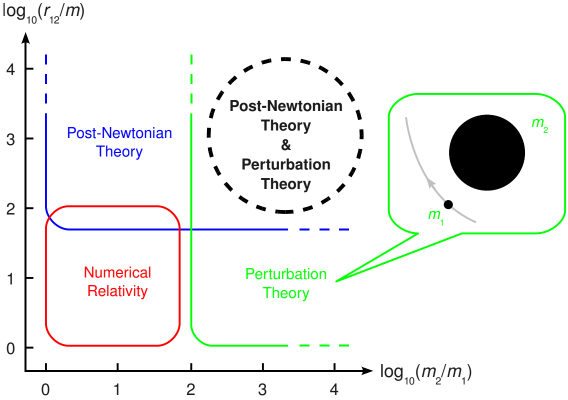

Methods to compute gravitational wave templates

Black hole perturbation theory and the gravitational self-force

Spacetime metric

$$g_{\mu\nu} = \bar{g}_{\mu\nu}$$

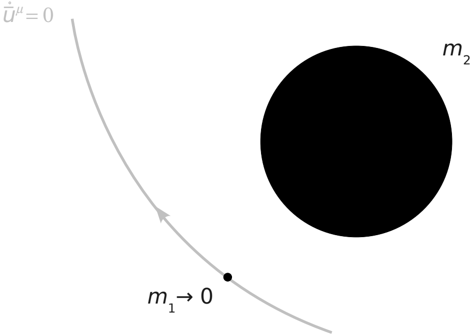

Methods to compute gravitational wave templates

Black hole perturbation theory and the gravitational self-force

Spacetime metric

$$g_{\mu\nu} = \bar{g}_{\mu\nu}$$

Perturbation parameter

$$q \equiv \frac{m_1}{m_2} \ll 1$$

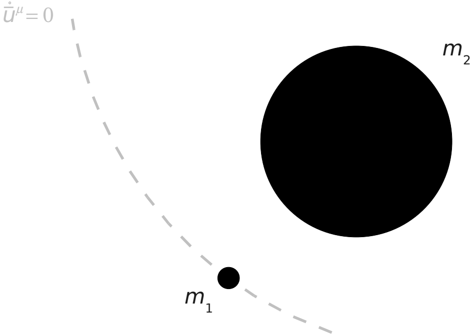

Methods to compute gravitational wave templates

Black hole perturbation theory and the gravitational self-force

Spacetime metric

$$g_{\mu\nu} = \bar{g}_{\mu\nu} + h_{\mu\nu}$$

Perturbation parameter

$$q \equiv \frac{m_1}{m_2} \ll 1$$

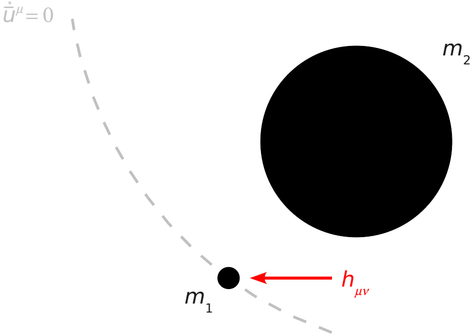

Methods to compute gravitational wave templates

Black hole perturbation theory and the gravitational self-force

Spacetime metric

$$g_{\mu\nu} = \bar{g}_{\mu\nu} + h_{\mu\nu}$$

Perturbation parameter

$$q \equiv \frac{m_1}{m_2} \ll 1$$

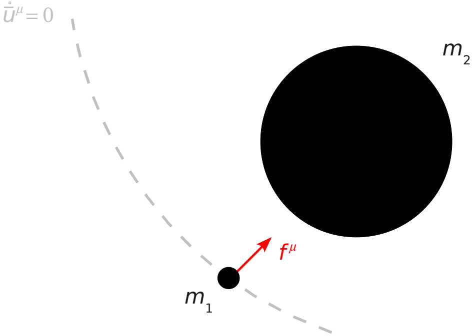

Methods to compute gravitational wave templates

Black hole perturbation theory and the gravitational self-force

Spacetime metric

$$g_{\mu\nu} = \bar{g}_{\mu\nu} + h_{\mu\nu}$$

Perturbation parameter

$$q \equiv \frac{m_1}{m_2} \ll 1$$

Self-force (SF) effect

$$\dot{\bar{u}}^{\mu} = f^{\mu} = \mathcal{O}(q)$$

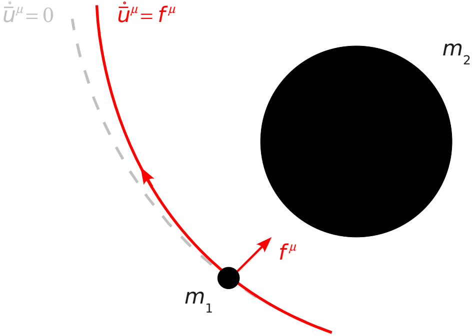

Methods to compute gravitational wave templates

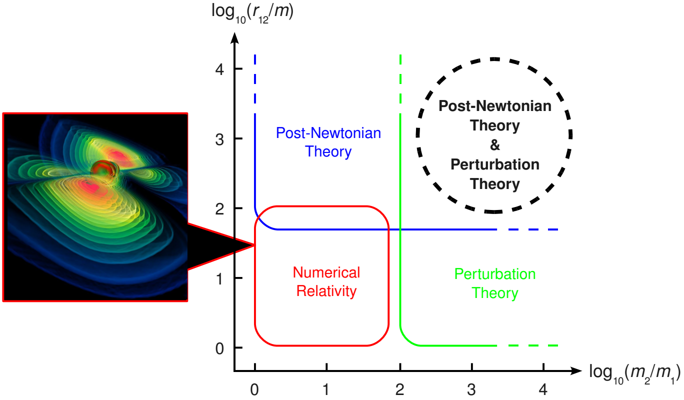

Methods to compute gravitational wave templates

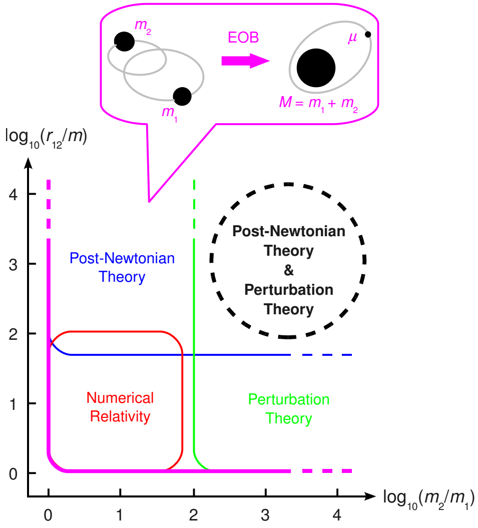

Methods to compute gravitational wave templates

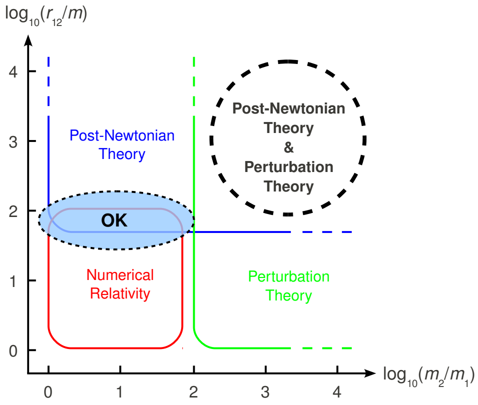

Methods to compute gravitational wave templates

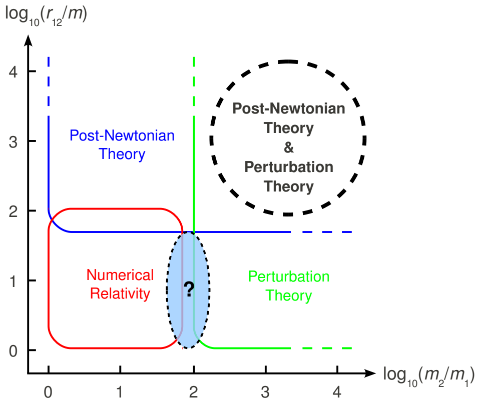

Methods to compute gravitational wave templates

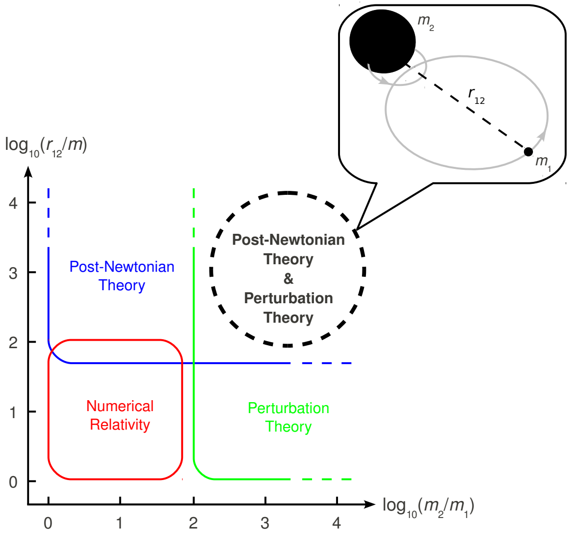

Outline

1. Gravitational wave source modelling
2. Post-Newtonian and self-force dynamics of black hole binaries
3. Cold dark matter and modified Newtonian dynamics
4. Dipolar dark matter and dark energy

How can a meaningful comparison be made?

- Conservative part of the dynamics only
- For circular orbits, the geometry admits an helical Killing vector k^α such that

$$k^\alpha = (\partial_t)^\alpha + \Omega\,(\partial_\varphi)^\alpha \quad \text{(asymptotically)}$$

- Four-velocity u^α of the particle necessarily tangent to the helical Killing vector:

$$u^\alpha = u^T k_1^\alpha$$

- Relation $u^T(\Omega)$ well defined in both PN and SF frameworks, and gauge invariant

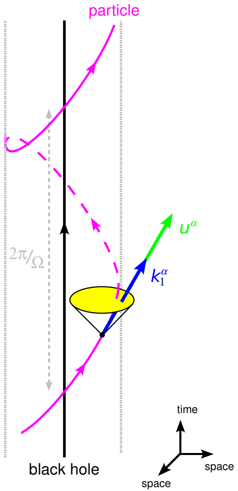

Post-Newtonian calculation of the "redshift observable"

$$u^t = \left(-g_{\alpha\beta}(\mathbf{y}_1) \, \frac{v_1^\alpha v_1^\beta}{c^2} \right)^{-1/2}$$

$\uparrow$ regularized metric at $\mathbf{y}_1$

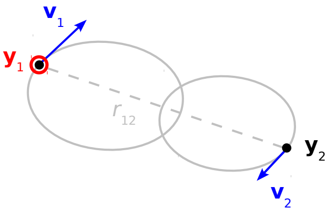

- Calculation of $g_{\alpha\beta}(\mathbf{x})$ at the location $\mathbf{x} = \mathbf{y}_1$ at 3PN order
- The metric is singular at the location of the particle
- It is regularized by means of dimensional regularization
- Computation of the 4PN and 5PN logarithmic contributions arising from gravitational wave tails

Post-Newtonian result for the SF effect on $u^t(\Omega)$

[Blanchet, Detweiler, Le Tiec & Whiting 10 (a,b)]

- The extreme mass ratio limit of u^t for circular orbits reads

$$u^t = u^t_{\text{Schw}} \underbrace{- q\, u^t_{\text{SF}}}_{\text{SF effect}} + q^2 u^t_{\text{PSF}} + \mathcal{O}(q^3)$$

Post-Newtonian result for the SF effect on $u^t(\Omega)$

[Blanchet, Detweiler, Le Tiec & Whiting 10 (a,b)]

- The extreme mass ratio limit of u^t for circular orbits reads

$$u^t = u^t_{\text{Schw}} \underbrace{- q\, u^t_{\text{SF}}}_{\text{SF effect}} + q^2 u^t_{\text{PSF}} + \mathcal{O}(q^3)$$

- Result expressed as a power series in $y \equiv \left(\frac{G m_2 \Omega}{c^3}\right)^{2/3} \sim \left(\frac{v}{c}\right)^2$

Post-Newtonian result for the SF effect on $u^t(\Omega)$

[Blanchet, Detweiler, Le Tiec & Whiting 10 (a,b)]

- The extreme mass ratio limit of u^t for circular orbits reads

$$u^t = u^t_{\mathrm{Schw}} \underbrace{- q\, u^t_{\mathrm{SF}}}_{\text{SF effect}} + q^2 u^t_{\mathrm{PSF}} + \mathcal{O}(q^3)$$

- Result expressed as a power series in $y \equiv \left(\frac{G m_2 \Omega}{c^3}\right)^{2/3} \sim \left(\frac{v}{c}\right)^2$
- Combining the results of our PN calculations, the SF effect is

$$u^t_{\mathrm{SF}}(y) = y + 2y^2 + 5y^3 + \overbrace{\left(\frac{121}{3} - \frac{41}{32}\pi^2\right) y^4}^{\text{3PN contribution}}$$
$$+ \Big(a_4 + \underbrace{\frac{64}{5}\ln y}_{\text{4PN log}}\Big) y^5 + \Big(a_5 \underbrace{- \frac{956}{105}\ln y}_{\text{5PN log}}\Big) y^6 + o(y^6)$$

High-precision comparison of the 3PN coefficient

- We fit the result of the SF calculation by a PN series

$$u^t_{\mathrm{SF}}(y) = \sum_{n\geqslant 0} a_n \, y^{n+1} + \ln y \sum_{n\geqslant 4} b_n \, y^{n+1}$$

High-precision comparison of the 3PN coefficient

- We fit the result of the SF calculation by a PN series

$$u^t_{\mathrm{SF}}(y) = \sum_{n\geqslant 0} a_n\, y^{n+1} + \ln y \sum_{n\geqslant 4} b_n\, y^{n+1}$$

- The known values of the coeff. $\{a_0, a_1, a_2\}$ up to 2PN are used, as well as the 4PN and 5PN logarithmic coeff. $\{b_4, b_5\}$

High-precision comparison of the 3PN coefficient

- We fit the result of the SF calculation by a PN series

$$u^t_{\mathrm{SF}}(y) = \sum_{n\geqslant 0} a_n\, y^{n+1} + \ln y \sum_{n\geqslant 4} b_n\, y^{n+1}$$

- The known values of the coeff. $\{a_0, a_1, a_2\}$ up to 2PN are used, as well as the 4PN and 5PN logarithmic coeff. $\{b_4, b_5\}$
- The fit of the numerical SF data yields for the 3PN coefficient

$$a_3^{\mathrm{SF}} = 27.6879034 \pm 0.0000004$$

High-precision comparison of the 3PN coefficient

- We fit the result of the SF calculation by a PN series

$$u^t_{\mathrm{SF}}(y) = \sum_{n\geqslant 0} a_n\, y^{n+1} + \ln y \sum_{n\geqslant 4} b_n\, y^{n+1}$$

- The known values of the coeff. $\{a_0, a_1, a_2\}$ up to 2PN are used, as well as the 4PN and 5PN logarithmic coeff. $\{b_4, b_5\}$
- The fit of the numerical SF data yields for the 3PN coefficient

$$a_3^{\mathrm{SF}} = 27.6879034 \pm 0.0000004$$

- The 3PN calculation with dimensional regularization gives

$$a_3 = \frac{121}{3} - \frac{41}{32}\pi^2 = 27.6879026\cdots$$

High-precision comparison of the 3PN coefficient

- We fit the result of the SF calculation by a PN series

$$u^t_{\mathrm{SF}}(y) = \sum_{n\geqslant 0} a_n\, y^{n+1} + \ln y \sum_{n\geqslant 4} b_n\, y^{n+1}$$

- The known values of the coeff. $\{a_0, a_1, a_2\}$ up to 2PN are used, as well as the 4PN and 5PN logarithmic coeff. $\{b_4, b_5\}$
- The fit of the numerical SF data yields for the 3PN coefficient

$$a_3^{\mathrm{SF}} = 27.6879034 \pm 0.0000004$$

- The 3PN calculation with dimensional regularization gives

$$a_3 = \frac{121}{3} - \frac{41}{32}\pi^2 = 27.6879026\cdots$$

- The two calculations are therefore in agreement at the 2σ level with 9 significant digits

High-order PN fit of the gravitational SF calculation

- Again we fit the result of the perturbative SF calculation by a PN series of the type

$$u^t_{\mathrm{SF}}(y) = \sum_{n\geqslant 0} a_n\, y^{n+1} + \ln y \sum_{n\geqslant 4} b_n\, y^{n+1}$$

High-order PN fit of the gravitational SF calculation

- Again we fit the result of the perturbative SF calculation by a PN series of the type

$$u^t_{\mathrm{SF}}(y) = \sum_{n\geqslant 0} a_n\, y^{n+1} + \ln y \sum_{n\geqslant 4} b_n\, y^{n+1}$$

- But this time we also use the known value of the 3PN coefficient a_3.

High-order PN fit of the gravitational SF calculation

- Again we fit the result of the perturbative SF calculation by a PN series of the type

$$u^t_{\mathrm{SF}}(y) = \sum_{n\geqslant 0} a_n\, y^{n+1} + \ln y \sum_{n\geqslant 4} b_n\, y^{n+1}$$

- But this time we also use the known value of the 3PN coefficient a_3. Our best fit yields:

PN order	coeff.	value
4	a_4	$+114.34747(5)$
5	a_5	$+245.53(1)$
6	a_6	$+695(2)$
6	b_6	$-339.3(5)$
7	a_7	$+5837(16)$

Comparison of the PN and SF calculations

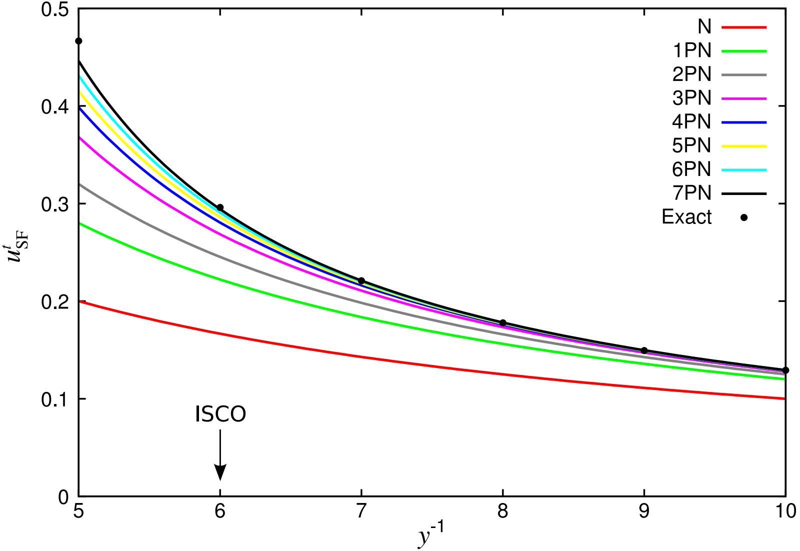

Summary and prospects

Successful comparison of the PN and SF formalisms:

- Impressive agreement between analytically determined PN coefficients and results from fit of numerical SF (e.g. 3PN)
- Extraction of previously unknown high-order PN coefficients (up to 7PN) from accurate SF data
- Confirms the adequacy of the regularization schemes used in both PN and SF approaches

Summary and prospects

Successful comparison of the PN and SF formalisms:

- Impressive agreement between analytically determined PN coefficients and results from fit of numerical SF (e.g. 3PN)
- Extraction of previously unknown high-order PN coefficients (up to 7PN) from accurate SF data
- Confirms the adequacy of the regularization schemes used in both PN and SF approaches

More comparisons to come in the future:

- Eccentric orbits in Schwarzschild
  [Barack, Le Tiec & Sago, in progress]
- Circular/eccentric (equatorial) orbits in Kerr
- Post-SF terms in the energy flux (2^{nd} order BH perturbations)

Outline

① Gravitational wave source modelling

② Post-Newtonian and self-force dynamics of black hole binaries

③ Cold dark matter and modified Newtonian dynamics

④ Dipolar dark matter and dark energy

The concordance model of cosmology or ΛCDM scenario

- Cosmic microwave background anisotropies
- Hubble diagram of supernovæ
- Baryonic acoustic oscillations
- Big Bang nucleosynthesis
- Weak and strong lensing
- Growth of structures
- Mass discrepancy
- ...

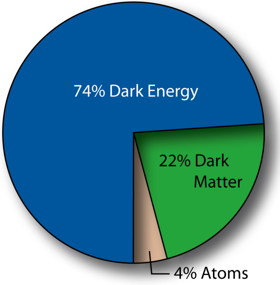

Galaxies are dominated by non-baryonic dark matter

- For a circular orbit in Newtonian gravity

$$V_{\text{rot}}(r) = \sqrt{\frac{GM(r)}{r}}$$

- The observation that $V_{\text{rot}} \simeq \text{cst.}$ requires

$$M_{\text{halo}}(r) \propto r$$

$$\rho_{\text{halo}}(r) \propto \frac{1}{r^2}$$

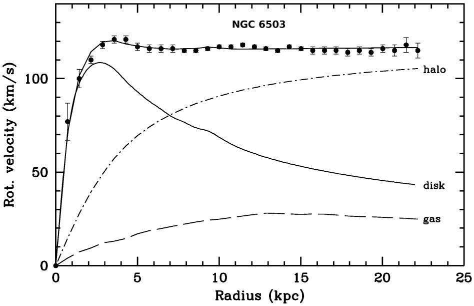

Figure: A spiral galaxy rotation curve [Bottema 97]

The pros and cons of cold dark matter (CDM)

✔ Independant motivation from particle physics [Bertone *et al.* 04]:

- Neutralino in MSSM
- Kaluza-Klein states
- ...

The pros and cons of cold dark matter (CDM)

✔ Independant motivation from particle physics [Bertone *et al.* 04]:

- Neutralino in MSSM
- Kaluza-Klein states
- ...

✔ Successfully applied at cosmological scales:

- Accounts for the observed mass discrepancies
- Triggers the formation of large-scale structures
- ...

The pros and cons of cold dark matter (CDM)

✔ Independant motivation from particle physics [Bertone *et al.* 04]:

- Neutralino in MSSM
- Kaluza-Klein states
- ...

✔ Successfully applied at cosmological scales:

- Accounts for the observed mass discrepancies
- Triggers the formation of large-scale structures
- ...

✘ Faces numerous challenges at galactic scales:
[Peebles & Nusser 10, Kroupa *et al.* 10]

- Core/cusp problem in central regions of galaxies
- Problem of missing satellites of large galaxies
- Galactic phenomenology, e.g. [McGaugh & Sanders 04]
    - Baryonic Tully-Fisher relation
    - Faber-Jackson relation
    - Milgrom's law
- ...

MOdified Newtonian Dynamics (MOND) [Milgrom 83]

- An alternative to the dark matter hypothesis
- No dark matter but violation of the fundamental law of gravity
- Designed to account for the phenomenology of the flat rotation curves of galaxies and the Tully-Fisher relation

- Modified Poisson equation

$$\nabla \cdot \left[\mu \left(\frac{g}{a_0} \right) \mathbf{g} \right] = -4\pi G \rho_b$$

- MOND acceleration scale

$$a_0 \simeq 1.2 \times 10^{-10} \text{ m/s}^2$$

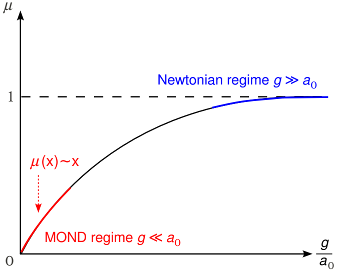

Many galactic rotation curves are fitted by MOND

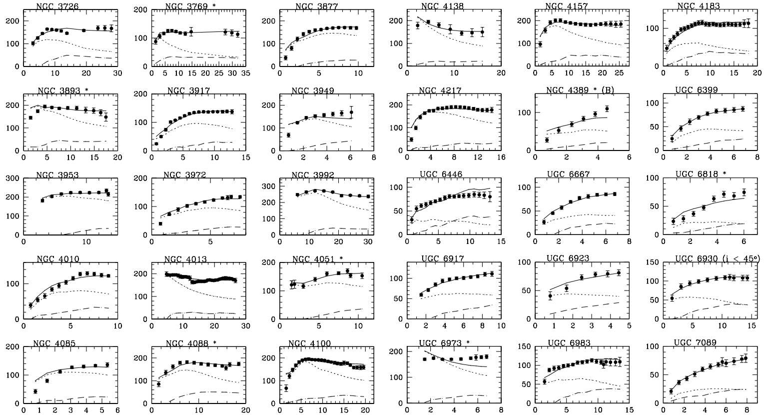

Figure: Rotation curves of Ursa Major galaxies [Sanders & Verheijen 98]

The pros and cons of MOND

✔ Accounts for numerous observations at the galactic scale: [McGaugh & Sanders 04]

- Baryonic Tully-Fisher relation
- One-parameter fit of galactic rotation curves
- Prediction of large mass discrepancy in dwarf spheroidals
- Bars in galaxies and galactic mergers [Combes & Tiret 10]
- ...

The pros and cons of MOND

✔ Accounts for numerous observations at the galactic scale: [McGaugh & Sanders 04]

- Baryonic Tully-Fisher relation
- One-parameter fit of galactic rotation curves
- Prediction of large mass discrepancy in dwarf spheroidals
- Bars in galaxies and galactic mergers [Combes & Tiret 10]
- ...

✔ Relativistic extensions have been proposed:

- TeVeS [Bekenstein 04; Sanders 05]
- BIMOND [Milgrom 10]

The pros and cons of MOND

✔ Accounts for numerous observations at the galactic scale: [McGaugh & Sanders 04]

- Baryonic Tully-Fisher relation
- One-parameter fit of galactic rotation curves
- Prediction of large mass discrepancy in dwarf spheroidals
- Bars in galaxies and galactic mergers [Combes & Tiret 10]
- ...

✔ Relativistic extensions have been proposed:

- TeVeS [Bekenstein 04; Sanders 05]
- BIMOND [Milgrom 10]

✘ Postulates an *ad hoc* modification of the fundamental law of gravity (or inertia)

The pros and cons of MOND

✔ Accounts for numerous observations at the galactic scale: [McGaugh & Sanders 04]

- Baryonic Tully-Fisher relation
- One-parameter fit of galactic rotation curves
- Prediction of large mass discrepancy in dwarf spheroidals
- Bars in galaxies and galactic mergers [Combes & Tiret 10]
- ...

✔ Relativistic extensions have been proposed:

- TeVeS [Bekenstein 04; Sanders 05]
- BIMOND [Milgrom 10]

✘ Postulates an *ad hoc* modification of the fundamental law of gravity (or inertia)

✘ Remaining mass discrepancy at the scale of galaxy clusters [Gerbal *et al.* 92; Pointecouteau & Silk 08]

Outline

1. Gravitational wave source modelling
2. Post-Newtonian and self-force dynamics of black hole binaries
3. Cold dark matter and modified Newtonian dynamics
4. Dipolar dark matter and dark energy

MOND as gravitational polarization [Blanchet 07]

- Maxwell-Gauss equation in dielectric media

$$\nabla \cdot \mathbf{E} = \frac{1}{\varepsilon_0}\Big(\sigma_{\text{free}} \underbrace{-\nabla \cdot \mathbf{P}}_{\substack{\text{polarized}\\ \text{charges}}}\Big) \quad \underset{\mathbf{P}\propto\mathbf{E}}{\Longleftrightarrow} \quad \nabla \cdot \left[\varepsilon_r\left(E\right)\mathbf{E}\right] = \frac{1}{\varepsilon_0}\sigma_{\text{free}}$$

MOND as gravitational polarization [Blanchet 07]

- Maxwell-Gauss equation in dielectric media

$$\nabla\cdot\mathbf{E}=\frac{1}{\varepsilon_0}\Big(\sigma_{\text{free}}\underbrace{-\nabla\cdot\mathbf{P}}_{\substack{\text{polarized}\\ \text{charges}}}\Big)\quad\underset{\mathbf{P}\propto\mathbf{E}}{\Longleftrightarrow}\quad\nabla\cdot\left[\varepsilon_{\text{r}}(E)\,\mathbf{E}\right]=\frac{1}{\varepsilon_0}\sigma_{\text{free}}$$

- Poisson and MOND equations

$$\nabla\cdot\mathbf{g}=-4\pi G\Big(\rho_{\text{b}}\underbrace{-\nabla\cdot\mathbf{\Pi}}_{\substack{\text{polarized}\\ \text{masses}}}\Big)\quad\underset{\mathbf{\Pi}\propto\mathbf{g}}{\Longleftrightarrow}\quad\nabla\cdot\left[\mu(g)\,\mathbf{g}\right]=-4\pi G\,\rho_{\text{b}}$$

MOND as gravitational polarization [Blanchet 07]

- Maxwell-Gauss equation in dielectric media

$$\nabla \cdot \mathbf{E} = \frac{1}{\varepsilon_0}\Big(\sigma_{\text{free}} \underbrace{-\nabla \cdot \mathbf{P}}_{\text{polarized charges}}\Big) \quad \underset{\mathbf{P} \propto \mathbf{E}}{\Longleftrightarrow} \quad \nabla \cdot [\varepsilon_r(E)\,\mathbf{E}] = \frac{1}{\varepsilon_0}\sigma_{\text{free}}$$

- Poisson and MOND equations

$$\nabla \cdot \mathbf{g} = -4\pi G\Big(\rho_b \underbrace{-\nabla \cdot \mathbf{\Pi}}_{\text{polarized masses}}\Big) \quad \underset{\mathbf{\Pi} \propto \mathbf{g}}{\Longleftrightarrow} \quad \nabla \cdot [\mu(g)\,\mathbf{g}] = -4\pi G\,\rho_b$$

- Build a relativistic **modified matter** model which recovers the phenomenology of MOND in the non-relativistic limit *via* the physical mechanism of gravitational polarization

Lagrangian of the dipolar fluid

[Blanchet & Le Tiec 08; 09]

$$L = -\sigma + J_\mu \dot{\xi}^\mu - \mathcal{W}(\Pi_\perp)$$

- Conserved current $J^\mu = \sigma u^\mu$
- Dipole moment variable ξ^μ
- Potential $\mathcal{W}$, function of the polarization field $\Pi_\perp = \sigma \xi_\perp$

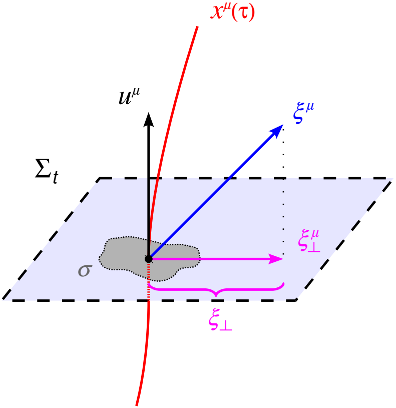

Link between dark energy and MOND

In the weak-field regime $g \ll a_0 \;\Leftrightarrow\; \Pi_\perp \ll a_0$

$$\mathcal{W}(\Pi_\perp) = \frac{\Lambda}{8\pi} + 2\pi\,\Pi_\perp^2 + \frac{16\pi^2}{3a_0}\,\Pi_\perp^3 + \mathcal{O}(\Pi_\perp^4)$$

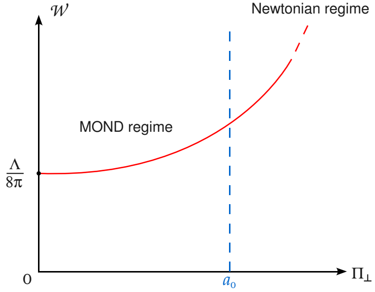

Link between dark energy and MOND

In the weak-field regime $g \ll a_0 \;\Leftrightarrow\; \Pi_\perp \ll a_0$

$$\mathcal{W}(\Pi_\perp) = \frac{\Lambda}{8\pi} + 2\pi\,\Pi_\perp^2 + \frac{16\pi^2}{3a_0}\,\Pi_\perp^3 + \mathcal{O}(\Pi_\perp^4)$$

- Dark energy as minimum of the potential when $\Pi_\perp = 0$

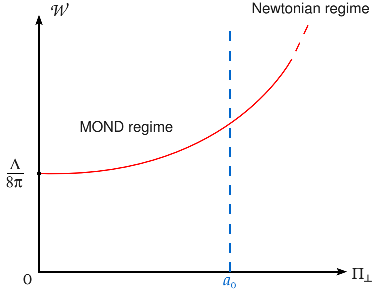

Link between dark energy and MOND

In the weak-field regime $g \ll a_0 \;\Leftrightarrow\; \Pi_\perp \ll a_0$

$$\mathcal{W}(\Pi_\perp) = \frac{\Lambda}{8\pi} + 2\pi\,\Pi_\perp^2 + \frac{16\pi^2}{3a_0}\,\Pi_\perp^3 + \mathcal{O}(\Pi_\perp^4)$$

- Dark energy as minimum of the potential when $\Pi_\perp = 0$
- Phenomenology of MOND in the non-relativistic limit

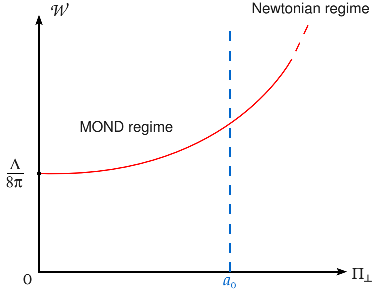

Link between dark energy and MOND

In the weak-field regime $g \ll a_0 \;\Leftrightarrow\; \Pi_\perp \ll a_0$

$$\mathcal{W}(\Pi_\perp) = \frac{\Lambda}{8\pi} + 2\pi\,\Pi_\perp^2 + \frac{16\pi^2}{3a_0}\,\Pi_\perp^3 + \mathcal{O}(\Pi_\perp^4)$$

- Dark energy as minimum of the potential when $\Pi_\perp = 0$
- Phenomenology of MOND in the non-relativistic limit

"Cosmic coincidence" that $\Lambda \sim a_0^2$ comes out naturally

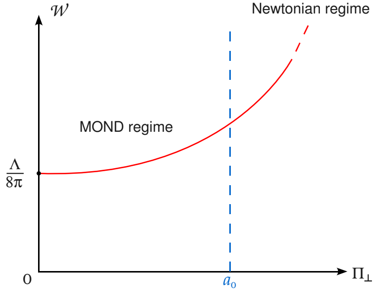

Recovering ΛCDM at cosmological scales

- Effective variables

$$\widetilde{u}^\mu = u^\mu + \mathscr{L}_{\xi_\perp} u^\mu$$
$$\rho = \sigma - \nabla_\lambda \Pi_\perp^\lambda$$

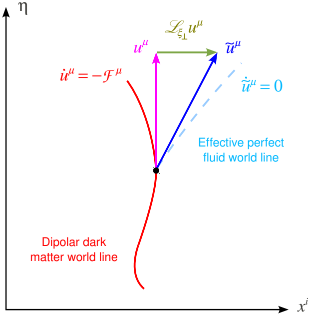

Recovering ΛCDM at cosmological scales

- Effective variables

$$\widetilde{u}^\mu = u^\mu + \mathscr{L}_{\xi_\perp} u^\mu$$
$$\rho = \sigma - \nabla_\lambda \Pi^\lambda_\perp$$

- Stress-energy tensor

$$T_{\mu\nu} = \underbrace{-\frac{\Lambda}{8\pi}\, g_{\mu\nu}}_{\text{dark energy}} + \underbrace{\rho\, \widetilde{u}_\mu \widetilde{u}_\nu}_{\text{cold dark matter}}$$

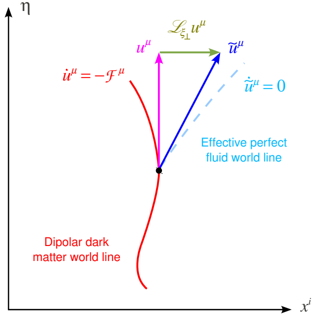

Recovering ΛCDM at cosmological scales

- Effective variables

$$\widetilde{u}^\mu = u^\mu + \mathscr{L}_{\xi_\perp} u^\mu$$
$$\rho = \sigma - \nabla_\lambda \Pi^\lambda_\perp$$

- Stress-energy tensor

$$T_{\mu\nu} = \underbrace{-\frac{\Lambda}{8\pi} g_{\mu\nu}}_{\text{dark energy}} + \underbrace{\rho\, \widetilde{u}_\mu \widetilde{u}_\nu}_{\text{cold dark matter}}$$

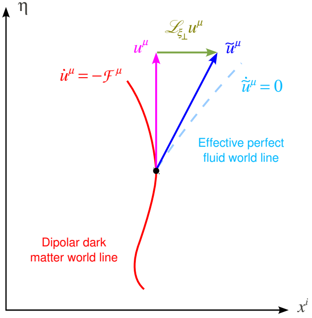

- The dipolar DM fluid is undistinguishable from standard CDM at the level of 1st order cosmological perturbations

Recovering ΛCDM at cosmological scales

- Effective variables

$$\widetilde{u}^\mu = u^\mu + \mathscr{L}_{\xi_\perp} u^\mu$$
$$\rho = \sigma - \nabla_\lambda \Pi^\lambda_\perp$$

- Stress-energy tensor

$$T_{\mu\nu} = \underbrace{-\frac{\Lambda}{8\pi} g_{\mu\nu}}_{\text{dark energy}} + \underbrace{\rho\, \widetilde{u}_\mu \widetilde{u}_\nu}_{\text{cold dark matter}}$$

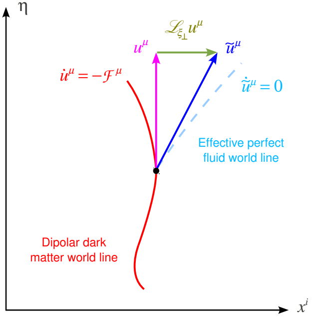

- The dipolar DM fluid is undistinguishable from standard CDM at the level of 1st order cosmological perturbations
- Adjusting $(\bar{\sigma}, \Lambda)$ so that $(\Omega_{\rm dm} \simeq 0.23, \Omega_{\rm de} \simeq 0.73)$, the model predicts the same spectrum of CMB temperature fluctuations

Recovering MOND at galactic scales

- Poisson equation in a galaxy

$$\nabla \cdot \mathbf{g} = -4\pi G \left(\rho_b + \underbrace{\sigma - \nabla \cdot \mathbf{\Pi}_\perp}_{\text{mass density } \rho_{dm}}\right)$$

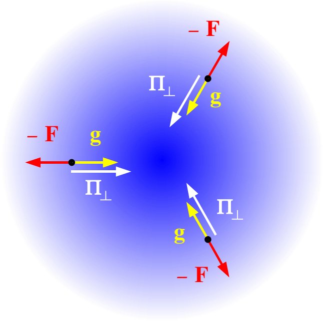

Recovering MOND at galactic scales

- Poisson equation in a galaxy

$$\nabla\cdot\mathbf{g} = -4\pi G\left(\rho_\mathrm{b} + \underbrace{\sigma - \nabla\cdot\mathbf{\Pi}_\perp}_{\text{mass density } \rho_\mathrm{dm}}\right)$$

- Weak Clustering Hypothesis ($\mathbf{v} \simeq \mathbf{0}, \sigma \ll \rho_\mathrm{b}$) implies

$$\mathbf{\Pi}_\perp = -\frac{\chi(g)}{4\pi G}\,\mathbf{g}$$

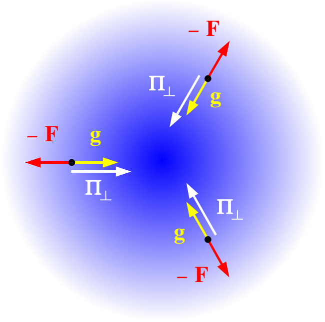

Recovering MOND at galactic scales

- Poisson equation in a galaxy

$$\nabla\cdot\mathbf{g} = -4\pi G\big(\rho_{\rm b} + \underbrace{\sigma - \nabla\cdot\mathbf{\Pi}_\perp}_{\text{mass density } \rho_{\rm dm}}\big)$$

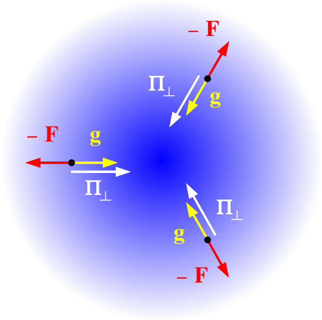

- Weak Clustering Hypothesis ($\mathbf{v}\simeq\mathbf{0}, \sigma \ll \rho_{\rm b}$) implies

$$\mathbf{\Pi}_\perp = -\frac{\chi(g)}{4\pi G}\,\mathbf{g}$$

- The dipolar DM then benefits from the various successes of the phenomenology of MOND at galactic scales

Recovering MOND at galactic scales

- Poisson equation in a galaxy

$$\nabla \cdot \mathbf{g} = -4\pi G \left(\rho_b + \underbrace{\sigma - \nabla \cdot \mathbf{\Pi}_\perp}_{\text{mass density } \rho_{dm}}\right)$$

- Weak Clustering Hypothesis ($\mathbf{v} \simeq \mathbf{0}, \sigma \ll \rho_b$) implies

$$\mathbf{\Pi}_\perp = -\frac{\chi(g)}{4\pi G}\,\mathbf{g}$$

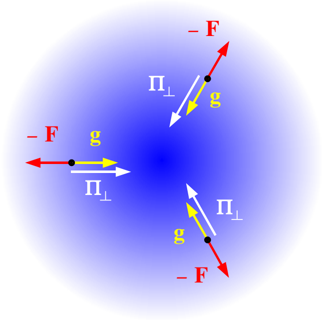

- The dipolar DM then benefits from the various successes of the phenomenology of MOND at galactic scales
- It provides a simple explanation for this phenomenology through the physical mechanism of polarization

Summary and prospects

This phenomenological model of dipolar dark matter:

- Is based on a simple and physically motivated matter Lagrangian in standard general relativity
- Is equivalent to ΛCDM at cosmological scales
- Recovers the phenomenology of MOND at galactic scales *via* the mechanism of gravitational polarization (modulo WCH)
- "Cosmic coincidence" that $\Lambda \sim a_0^2$ is a natural outcome

Summary and prospects

This phenomenological model of dipolar dark matter:

- Is based on a simple and physically motivated matter Lagrangian in standard general relativity
- Is equivalent to ΛCDM at cosmological scales
- Recovers the phenomenology of MOND at galactic scales *via* the mechanism of gravitational polarization (modulo WCH)
- "Cosmic coincidence" that $\Lambda \sim a_0^2$ is a natural outcome

Further connections with observations:

- Non-gaussianities in the CMB temperature anisotropies
  [Blanchet, Langlois, Le Tiec & Marsat, in progress]
- Non-linear growth of density perturbations using numerical simulations (test the WCH)
- Stochastic background of gravitational radiation

EXTRA SLIDES

PN equations of motion for compact binaries

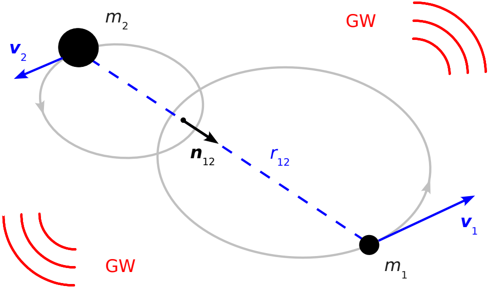

$$\frac{\mathrm{d}\mathbf{v}_1}{\mathrm{d}t} = \underbrace{-\frac{Gm_2}{r_{12}^2}\mathbf{n}_{12} + \frac{\mathbf{A}_{1PN}}{c^2} + \frac{\mathbf{A}_{2PN}}{c^4}}_{\text{conservative terms}} + \underbrace{\frac{\mathbf{A}_{2.5PN}}{c^5}}_{\text{rad. reac.}} + \underbrace{\frac{\mathbf{A}_{3PN}}{c^6}}_{\text{cons. term}} + \underbrace{\frac{\mathbf{A}_{3.5PN}}{c^7}}_{\text{rad. reac.}} + \cdots$$

Dimensional regularization: a simple example

- Time component of the Newtonian metric in $d = 3$ space dimensions

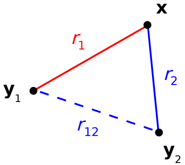

$$g_{00}(\mathbf{x}) = -1 + \frac{2Gm_1}{c^2 r_1} + \frac{2Gm_2}{c^2 r_2} + \cdots$$

- Not defined at the location $\mathbf{y}_1$ in the limit $r_1 \to 0$
- Time component of the metric in d space dimensions

$$g_{00}^{(d)}(\mathbf{x}) = -1 + \frac{2G^{(d)} m_1}{c^2 r_1^{d-2}} + \frac{2G^{(d)} m_2}{c^2 r_2^{d-2}} + \cdots$$

- Analytic continuation in the space dimension: $d \in \mathbb{C}$
- Choose $\mathcal{R}(d) < 2$ such that $g_{00}^{(d)}$ is defined in the limit $r_1 \to 0$
- Relying on the uniqueness of analytic continuation, the 3-dimensional result is

$$g_{00}(\mathbf{y}_1) = \underset{d \to 3}{\text{AC}} \left[\lim_{\mathbf{x} \to \mathbf{y}_1} g_{00}^{(d)}(\mathbf{x}) \right] = -1 + \frac{2Gm_2}{c^2 r_{12}} + \cdots$$

Hereditary contribution from gravitational wave tails

- Gravitational radiation is scattered by the background curvature generated by the mass M of the source

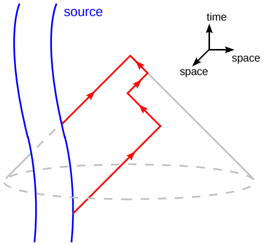

- Starting at 4N order, the near-zone metric depends on the entire past "history" of the source [Blanchet & Damour 88]

$$\delta g_{00}^{\text{tail}}(\mathbf{x},t) = -\frac{8G^2M}{5c^{10}}x^a x^b \int_{-\infty}^{t} \mathrm{d}t'\, M_{ab}^{(7)}(t') \ln\left(\frac{c(t-t')}{2r}\right)$$

Recoil as computed by numerical relativity (NR)

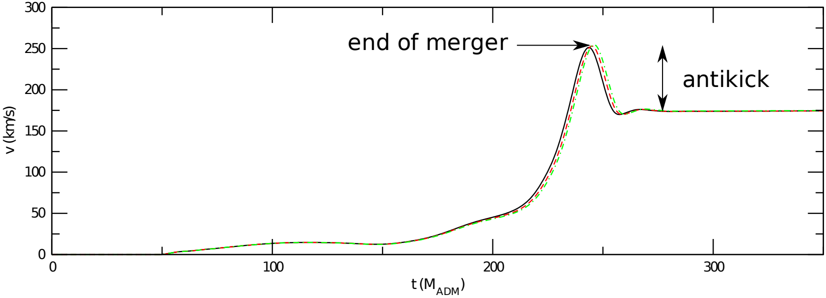

Figure: Numerical simulation ($\eta = 0.19$) [González *et al.* 07]

- Previous analytical estimate agrees with NR up to merger [Blanchet, Qusailah & Will 05]
- Does the "antikick" come from the ringdown phase?

Recoil velocity of coalescing black hole binaries